78. On-field spray downwash characterisation and comparison of Agras T10 and T50 UAV for spray application

A. Pagliai*, D. Sarri, C. Perna, C. Russo, N. Rimbotti, R. Lisci and M. Vieri
*Department of Agriculture, Food, Environment and Forestry, University of Florence, Piazzale delle Cascine 15 - 50144 Florence, Italy; * andrea.pagliai@unifi.it*

Abstract

The study tested the effect of different flight and spraying parameters of the commercial unmanned aerial vehicles (UAVs) DJI Agras T10 and T50 on spray downwash. The aim was to enable precision spray path planning by analysing the spatial spray distribution and swaths produced by the UAVs. The results showed an inhomogeneous droplet density distribution along the spray swath. The droplet distribution showed higher droplet density below the rotor-nozzle lines, highlighting the presence of two peaks. The higher forward speeds (4 and 5.6 m/s) and higher flight altitudes (2.5 and 3 m) reduced the peaks intensity and produced a more uniform spray swath. The average spray swath of the Agras T50 platform was slightly wider (3.5–4.5 m) than that of the Agras T10 (2.5–3.5 m), depending on the different flight and spraying parameters.

Keywords: spray distribution, spray swath, UASS, UAV settings, water-sensitive paper

Introduction

In recent years, the utilization of unmanned aerial vehicles (UAVs) in agriculture has grown increasingly widespread (Del Cerro *et al*., 2021). Concerning the application of agricultural inputs such as plant protection products (PPPs), seeding and fertilisers, unmanned aerial spraying systems (UASSs) represent a transformative advancement in precision agriculture. These systems have been shown to effectively address operational challenges in crop protection, particularly in complex high-slope scenarios or wet surfaces (Biglia *et al*., 2023; Wang *et al*., 2018). Nonetheless, aerial pesticide spraying is outlawed in Europe through European directive 2009/128/EC, leading to diminished competitiveness in research within this domain and, more generally, in technology transfer to farmers. As a result, UASSs have been developed and are presently utilized mostly in the Americas and Asia. China is estimated to have deployed around 10 000 UAV spray systems, covering more than 2 Mha (He *et al*., 2017).
In this context, several studies have recently been conducted with the objective of identifying the operational parameters of UAVs that have the greatest impact on spray application, and simultaneously, to ascertain the optimal flight and spray attributes for enhancing spray deposition efficiency (Biglia *et al*., 2023; Sánchez-Fernández *et al*., 2024). Nevertheless, only a limited number of these studies have employed the use of commercially available UASSs (Wang *et al*., 2024). Furthermore, to the best of the authors' knowledge, no study has been conducted on the DJI Agras T50 in Europe to characterise the spray downwash, since it was launched on the European market in April 2024. Under these circumstances the objective of this study was twofold. Firstly, to characterise two commercial UAVs (DJI Agras T10 and T50) on-field spray distribution by analysing water-sensitive papers at varying forward UAV speeds (2, 3, 4 and 5.6 m/s), flight altitudes (2, 2.5 and 3 m) and nozzles (flat-cone XR11002VS and rotative-nozzle LX8060SZ). Secondly, to compare the spray downwashes to optimise spray practices and enhance the efficiency and effectiveness of UAV applications in precision crop protection.

Materials and methods

The experimentation was conducted at two distinct locations: one situated in Lastra a Signa (Florence, Italy) and the other in Colverde (Como, Italy). The experiments were carried out in two different years, 2023 and 2024 and with two different UAVs (Agras T10 and T50, DJI, Shenzhen, P.R. China). The two sites exhibited comparable meteorological and morphological conditions, as the experiments were conducted during the same period (June 2023 and 2024) and the UASSs were operated in a flat field that had undergone minimal ploughing. The three replications of the experimental design were represented by three wooden sampling lines placed in the field, placed at 10 m intervals. (Figure 1). At each interval, water-sensitive papers (WSP, 26×76 mm, Syngenta Crop Protection, Basel, Switzerland) were affixed to characterize the spray distribution of the respective UAV. The length of the sampling lines and the distance between the water-sensitive papers were varied for each platform to ensure the spray swath was fully sampled. The sampling lines were 8 m long for the Agras T10 and 12 m long for the Agras T50, reflecting the differing dimensions of the UASSs and the subsequent anticipated differences in spray swaths. In the T10 experimental trials, the WSPs were positioned at 0.15 m from one another, while in the T50 trials, they were placed at 0.25 m from each other, as is illustrated in Figure 1.

The trials conducted in June 2023 were carried out with the DJI Agras T10 UAV (DJI, Shenzhen, China). The DJI Agras T10 is a quadrotor UAV that features an 8-litre spray tank and four nozzles positioned at 0.25 m beneath each rotor. The UAV is equipped with two diaphragm pumps, each of which powers two nozzles. This allows the flow rates of two or four nozzles to be combined, thereby generating a wide variety of flow rates. The distance between the front and rear nozzles is 990 mm, while the distance between the side nozzles is 1095 mm. In contrast, the trials conducted in June 2024 employed the DJI Agras T50 UAV (DJI). The DJI Agras T50 is equipped with four rotor shafts and a coaxial twin-rotor propulsion system for each shaft. The spraying system is equipped with a 40-litre tank for liquid, two rotative nozzles (LX8060SZ, DJI) located at 0.45 m below the rear twin rotors and two centrifugal pumps with a maximum flow rate of 16 l/min. In terms of functionality, the rotative nozzles facilitate the variation of droplet dimensions from 50 to 500 μm in accordance with the revolution per minute of the nozzle plate. The lateral wheelbase between the nozzles is 1570 mm, while the forward-backward wheelbase is 1425 mm.

In order to characterise and compare the spray field downwash of the T10 and T50 UAVs, eight experimental trials were conducted for each UAV, with the main influencing factors, including forward speed, flight height and nozzles, being varied. An experimental trial is defined as a single path of the UAV flight, perpendicular to and centred on the sampling lines. The various parameters

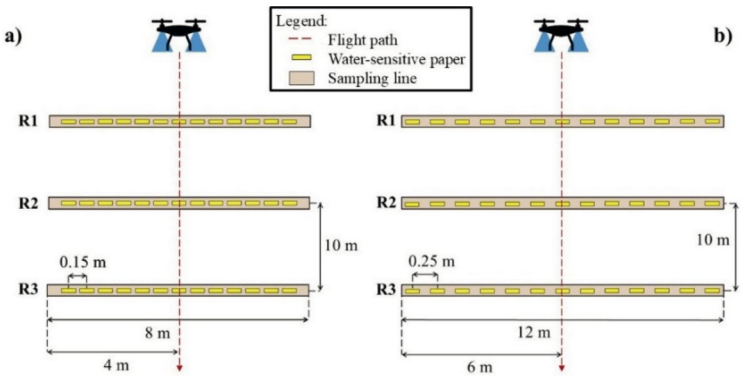

Figure 1. Experimental layout for Agras T10 (a) and for Agras T50 (b).

Table 1. Different parameters set in experimental tests.

Test	UAV	Flight height (m)	Spray volume (l/ha)	Flight speed (m/s)	Nozzle
A1	T10	2	30	2	XR 11002 VS
A2	T10	2.5	30	2	XR 11002 VS
A3	T50	2.5	30	2	LX 8060 SZ
A4	T50	3	30	2	LX 8060 SZ
B1	T10	2	30	3	XR 11002 VS
B2	T10	2.5	30	3	XR 11002 VS
B3	T50	2.5	30	3	LX 8060 SZ
B4	T50	3	30	3	LX 8060 SZ
C1	T10	2	30	4	XR 11002 VS
C2	T10	2.5	30	4	XR 11002 VS
C3	T50	2.5	30	4	LX 8060 SZ
C4	T50	3	30	4	LX 8060 SZ
D1	T10	2	30	5.6	XR 11002 VS
D2	T10	2.5	30	5.6	XR 11002 VS
D3	T50	2.5	30	5.6	LX 8060 SZ
D4	T50	3	30	5.6	LX 8060 SZ

that were tested are presented in Table 1. It should be noted that the experimental design is not fully factorial as the spraying systems on the different UASSs are not interchangeable, and the Agras T50 is not capable of flying at a similar altitude to the Agras T10 due to technical limitations. In particular, two flight heights from the ground for each UAV (2–2.5 m for Agras T10 and 2.5–3 for Agras T50), four flight speeds (2, 3, 4 and 5.6 m/s) and two type of nozzles (XR11002VS, Teejet Technologies, Glendale Heights, IL, USA; LX8060SZ, DJI). Regarding droplet dimensions, each trial was conducted with the objective of obtaining a medium droplet spectrum dimension, in accordance with the ISO standard 25358. During each trial, the main meteorological variables (air temperature, air humidity, wind speed and direction) were monitored at a height of 2 m using a 2900ET Watchdog Weather Station (Spectrum Technologies, Aurora, IL, USA). Concerning the weather conditions, the mean air temperature was 23.95°C and 25.83°C, mean relative humidity 44.5% and 42.1%, average wind speed recorded in each trial was always below 0.43 and 0.35 m/s, respectively, for Agras T10 and T50 tests.

After the spraying of each trial, WSPs were attached to labelled sheets for subsequently scanning by a multi-function printer (Kyocera TASKalfa 3554ci, Schiphol-Rijk, Netherlands) at 600 dpi upon arrival at the laboratory. Subsequently, the digital images of WSPs were analysed using the ImageJ software (v. 1.38x) to extract the spray coverage (%), the droplets density (droplets cm^{-2}) and the droplet size distribution (Dv.1, Dv.5, Dv.9). The droplets density (main variable) was analysed using the open-source software R (R Core Team, v 4.4.0-2024). Generalized additive models (GAMs) were used to model the data due to their non-linearity (Hastie and Tibshirani, 1986). The variable was modelled as a scaled t distribution of the sampling positions for each test. To obtain a good model fitting, the basis functions value was set to 33 for Agras T10 trials and to 20 for Agras T50. For both datasets (Agras T10 and T50), the smoothing parameter was estimated by the restricted maximum likelihood method (REML). The quality of the models was analysed through a combination of visual and statistical techniques. The visual assessment included the use of the quantile-quantile (Q-Q) plot, the histogram of residuals and the plot of the response versus the fitted values. Finally, the "ggplot2" package was used to graphically visualise the results.

Results and discussion

The outcomes of the GAM analyses regarding smoothing parameters and model residuals are presented in Table 2. To prevent overfitting or underfitting, the k parameter (number of basis functions) was set at 33 and at 20 in modelling the droplet density variable for the Agras T10 and Agras T50 trials, respectively. The discrepancy between the k-parameters employed in the T10 and T50 data modelling can be attributed to the specific experimental design. In fact, 53 and 45 WSPs were placed in each sampling line, resulting in a reduced requirement for basis functions to accurately model the data. Table 2 additionally presents the smoothing parameters derived from REML estimation. The variability between the replications was considered into smoothing parameter and managed through basis functions and REML estimation. The Ref.df and Chi.sq columns denote test statistics utilized to evaluate the overall significance of the smooth. The outcomes of these tests are displayed in the initial column of p-values. The test findings demonstrate that all smooths are statistically significant, hence validating the need for a smoothing modelling approach. The R^2 values are utilized to evaluate the model's quality and reliability. Most models demonstrate a high level of reliability in data representation, with an R^2 value of no less than 0.65, excepted for the B2 and D3 trials. However, even if these two trials have lower R^2 they are modelled by the GAM analysis with a good rate of reliability. The last two columns display the k-index and the p-value, which serve as statistical tests for patterns in model residuals. In this case, the high p-value (p>0.05) indicates that the residuals are randomly distributed.

Only the droplet density data from each experimental trial are shown in Figure 2 in the form of smoothing functions, as the trends were found to be like the coverage variable. This was because an ultra-low spray volume was used, which implies a linear relationship between the droplet density and the coverage. The smoothing curves are grouped according to similar flight speeds, with each curve (solid, dotted, dot-dash, and dashed lines) representing a single trial, as illustrated in Table 1. The results generally revealed two-peaked curves for both T10 and T50 UAVs, which exhibited flattening

Table 2. GAM outputs of droplet density model-fitting according to the trials.

Test	*k*	REML	EDF	Ref.df	χ^2	*p*-value	R^2	*k*-index	*p*-value
A1	33	641.1	17.8	20.7	3042	$<2e^{-16}$	0.880	1.23	1
A2	33	562.1	24.2	26.9	26701	$<2e^{-16}$	0.878	0.97	0.28
A3	20	494.3	12.1	13.4	1526	$<2e^{-16}$	0.756	1.06	0.74
A4	20	456.1	13.9	15.3	4489	$<2e^{-16}$	0.846	1.13	0.94
B1	33	488.8	14	16.4	1212	$<2e^{-16}$	0.784	0.95	0.39
B2	33	601.8	13.6	16.3	1856	$<2e^{-16}$	0.557	1.18	0.99
B3	20	476.8	11.8	13.5	1641	$<2e^{-16}$	0.817	1.18	0.97
B4	20	480.98	11.3	12.8	2373	$<2e^{-16}$	0.805	1.34	1
C1	33	559.2	19.4	21.9	19064	$<2e^{-16}$	0.905	1.15	0.96
C2	33	510.1	17.9	20.8	1784	$<2e^{-16}$	0.902	1.08	0.82
C3	20	436.3	13.1	14.7	2256	$<2e^{-16}$	0.820	1.14	0.97
C4	20	427.3	12.1	13.5	2359	$<2e^{-16}$	0.875	1.1	0.81
D1	33	463.6	10	12.2	668	$<2e^{-16}$	0.802	1.19	0.99
D2	33	465.8	7.8	9.6	299	$<2e^{-16}$	0.654	1.26	1
D3	20	483.9	8.5	9.9	337	$<2e^{-16}$	0.474	1.19	1
D4	20	404.7	10.9	12.5	566.4	$<2e^{-16}$	0.673	1.16	0.97

as the flight speed increased from 2 to 5.6 m/s. The increase in flight speed therefore caused an increase in the airflow generated by the rotors, which affected the distribution of the droplets, both by increasing the droplet density on the tails of the models, and by increasing the spray losses due to drift (Tang *et al*., 2023). The occurrence of each peak is observed to be below each nozzle-rotor system, thereby indicating a lack of homogeneity in the spray deposition. In particular, the two-peak phenomenon is more pronounced in the T10 UAV trials, particularly at lower speeds. In contrast, the two-peaks observed in the T50 UAV trials appear to be more flattened than the T10 data. This discrepancy could be attributed to the different nozzle system and layout present in the two UAVs. The rotative nozzles in the T50 UAV generate a radial droplet discharge that is more susceptible to the downwash produced by the propellers, resulting in a flattening of the peaks, and have wider opening angle that enlarge the droplet deposition cone.

Regarding the trials conducted at the same flight speed, an increase in flight height of the T10 UAV (from 2 to 2.5 m) has been observed to result in a reduction in the peaks of the droplet density, while simultaneously enlarging the spray swath. This finding is consistent with the results reported by Wang *et al.* (2024). However, the same effect was not observed in trials of the T50 UAV (from 2.5 to 3 m) about both the reduction of the droplet density peaks and the enlarging of the spray swath. The reason for this discrepancy is not fully understood. It may be due to the different flight heights tested with the two UAVs (T10, 2, 2.5 m; T50, 2.5, 3 m) or to the different nozzle system (T10, flat cone; T50, rotative nozzle). It should be noted that it was not possible to test the same flight height due to the T50 UAV's inability to fly at the same low altitude as the T10 UAV, which is a consequence of their differing dimensions.

Moreover, another important aspect to emphasise is the tails of droplet density models. The tails of droplet density models are indeed flattened at lower altitudes, which means low droplet density in the tails, resulting in a compact spray swath and reduced spray drift. In contrast, enlarging the spray swath at higher flight altitudes or higher flight speeds increases the droplet density in the tails of the models, causing the spray drift.

In addition, the minimum droplet density thresholds for effective pest and weed control provided by Syngenta Crop Protection (Pagliai *et al*., 2023) have been plotted as horizontal lines in the graphs in Figure 2 (magenta, fungicide threshold; green, herbicide threshold; brown, insecticide threshold) in order to compare the spatial deposition of droplets by the UAVs tested in terms of theoretical pesticide efficacy. The two peaks of the models generated by the Agras T10, particularly at the lower flight speeds tested (2, 3 and 4 m/s) and lower flight heights (2 m), resulted in the minimum fungicide thresholds being reached for most of the spray swath. In most cases, the gap in droplet deposition between the two peaks of the droplet density models produced by the T10 UAV, left the central part of the spray swath without a sufficient droplet density to meet the fungicide minimum threshold. Instead, the models produced by the Agras T50 only met the fungicide minimum threshold in a small number of trials (A3 and A4) and for a limited portion of the spray swath. This can be attributed to the lower peaks in droplet density generated by the T50 UAV, which tend to produce less irregular droplet density models.

Table 3 presents the spray swaths for each experimental trial, delineated according to the established thresholds for insecticides, herbicides, and fungicides. In general, the mean spray swath of the Agras T50 is slightly wider (3.5–4.5 m) than that of the Agras T10 (2.5–3.5 m). This attitude reflects the maximum size of the UAVs, given that the Agras T50 is 500 mm wider in every direction. These findings are consistent with the results reported by Biglia *et al.* (2023) and Wang *et al.* (2024), who performed similar trials, but strongly contrasts with the technical information provided by the producer in its operative manual, given that a maximum spray swath of 11 m was declared. In terms of spatial distribution uniformity and spray swath, the combination of high forward speed and high flight height resulted in a more uniform distribution than that achieved with low speed and low altitude. Nevertheless, in numerous instances, the droplet density did not attain the minimum requisite to guarantee crop protection in the overall spatial distribution of droplet density, or in some instances, in the central portion of the spatial distribution (as indicated in parentheses in Table 3), particularly regarding the fungicide threshold and in conjunction with Agras T50.

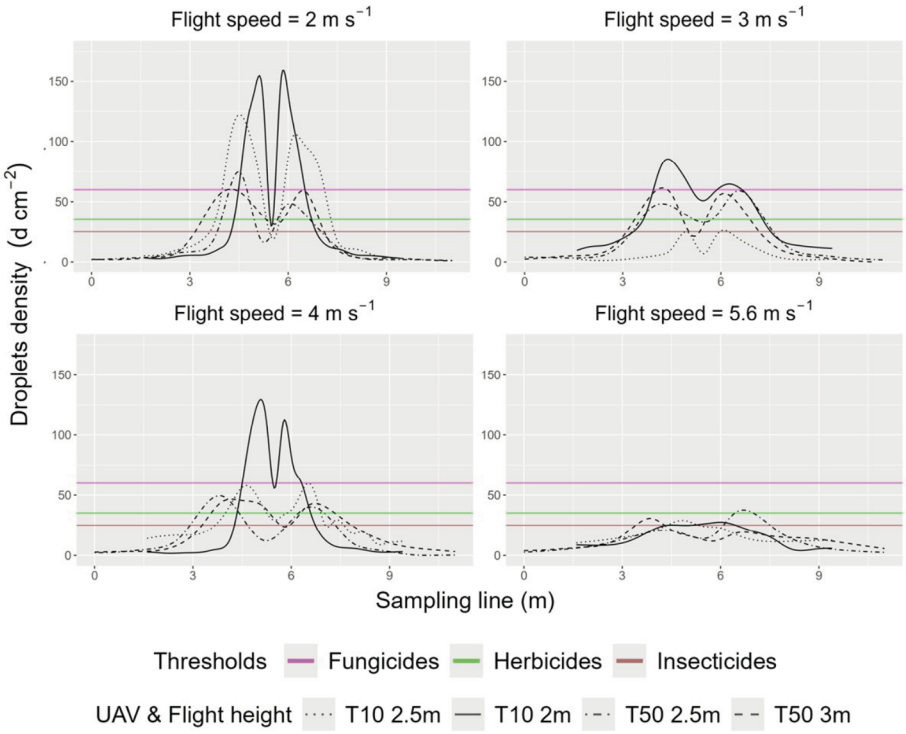

Figure 2. Spatial distribution of droplet density models in the experimental trials.

Table 3. Spray swaths for each experimental trials according to minimum droplet density thresholds of pesticide.

Test	A1	A2	A3	A4	B1	B2	B3	B4	
Insecticides	2.6	3.8	3.2 (0.5)	3.9	4.2	0.3	4.3	4.1 (0.3)	m
Herbicides	2.4	3.5 (0.5)	2.7 (0.7)	3.6 (0.5)	3.6	NR	3.8 (0.6)	3.5 (0.7)	m
Fungicides	2	3.1 (0.7)	0.5	2.4 (2)	2.7	NR	NR	0.3	m
Insecticides	2.4	3.4	4.4 (1.2)	4.6 (0.3)	2.1	1	1.4	0.9	m
Herbicides	2.2	2.9	3.9 (1.8)	3.8 (1)	NR	NR	0.6	NR	m
Fungicides	1.8	0.2	NR	NR	NR	NR	NR	NR	m
Test	C1	C2	C3	C4	D1	D2	D3	D4	

The spray gaps in the swaths are shown in parentheses and the pesticide threshold not reached is shown as NR (not reached).

Conclusions

The objective of this study was to evaluate the impact of selected flight and spray parameters on the characterisation of the spray downwash of two commercial UAVs. Furthermore, the study aimed to compare the spray downwashes to extract useful information for the precision path planning

and spray settings. According to the results of this study, the average spray swath of the Agras T50 was slightly wider (3.5–4.5 m) than that of the Agras T10 (2.5–3.5 m), which is more due to the size of the UAVs than to the flight altitudes tested. The UAVs generated similar spray downwashes, characterized by a two-peaks model of spray spatial distribution. In general, the peaks generated by T50 UAV are less prominent and wider rather than that of T10. All that is strongly influenced by the increase of the flight speed, reducing the prominence of the peaks and the increase of flight height, enlarging the spray swaths. In conclusion, in vine cultivation with a vertical training system, it should be better to take advantage of the two peaks of the models, localising them on the canopy, with the aim of reaching the threshold of fungicide products and contrasting off-target spraying. In contrast, for herbaceous crops, it is essential to ensure the greatest possible uniformity in the spatial distribution to enhance the efficiency of spraying, given that herbicides have lower efficacy thresholds. Therefore, the tangible outcomes demonstrated in this study provide a basis for the integration of UAVs into farmers' crop protection strategies, facilitating precision spraying with UASS.

References

Biglia, A., Grella, M., Comba, L., Sopegno, A., Eloi Alcatrão, L., Ricauda Aimonino, D., & Gay, P. (2023). Spray swath study in relation to canopy deposition during UAV spray applications in vineyards. In V. Ferro, G. Giordano, S. Orlando, M. Vallone, G. Cascone, & S.M.C. Porto (eds), AIIA 2022: Biosystems Engineering Towards the Green Deal, Vol. 337. Springer International, Cham, , pp. 345–352. https://doi.org/10.1007/978-3-031-30329-6_35

Del Cerro, J., Cruz Ulloa, C., Barrientos, A., & De León Rivas, J. (2021). Unmanned aerial vehicles in agriculture: a survey. Agronomy, 11(2), 203. https://doi.org/10.3390/agronomy11020203

Grella, M., Gioelli, F., Marucco, P., Zwertvaegher, I., Mozzanini, E., Mylonas, N., Nuyttens, D., & Balsari, P. (2022). Field assessment of a pulse width modulation (PWM) spray system applying different spray volumes: duty cycle and forward speed effects on vines spray coverage. Precision Agriculture, 23(1), 219–252. https://doi.org/10.1007/s11119-021-09835-6

Hastie, T., & Tibshirani, R. (1986). Generalized Additive Models. Statistical Science, 1(3). https://doi.org/10.1214/ss/1177013604

He, X., Bonds, J., Herbst, A., & Langenakens, J. (2017). Recent development of unmanned aerial vehicle for plant protection in East Asia. International Journal of Agricultural and Biological Engineering, 10(3), 18–30.

Pagliai, A., Sarri, D., Perna, C., & Vieri, M. (2023). Can a variable-rate sprayer be efficient and economic? testing and economic analysis in viticulture. In V. Ferro, G. Giordano, S. Orlando, M. Vallone, G. Cascone, & S.M.C. Porto (eds), AIIA 2022: Biosystems Engineering Towards the Green Deal. Springer International, Cham, pp. 805–815. https://doi.org/10.1007/978-3-031-30329-6_82

Sánchez-Fernández, L., Barrera-Báez, M., Martínez-Guanter, J., & Pérez-Ruiz, M. (2024). Reducing environmental exposure to PPPs in super-high density olive orchards using UAV sprayers. Frontiers in Plant Science, 14, 1272372. https://doi.org/10.3389/fpls.2023.1272372

Tang, Y., Fu, Y., Guo, Q., Huang, H., Tan, Z., & Luo, S. (2023). Numerical simulation of the spatial and temporal distributions of the downwash airflow and spray field of a co-axial eight-rotor plant protection UAV in hover. Computers and Electronics in Agriculture, 206, 107634. https://doi.org/10.1016/j.compag.2023.107634

Wang, G., Li, X., Andaloro, J., Chen, P., Song, C., Shan, C., & Lan, Y. (2018). Deposition and biological efficacy of UAV-based low-volume application in rice fields. International Journal of Precision Agricultural Aviation, 1(1), 65–72. https://doi.org/10.33440/j.ijpaa.20200302.86

Wang, S., Van Beek, J., Van Gehuchten, A., Zwertvaegher, I., & Nuyttens, D. (2024). Lab and field evaluation of a DJI Agras T10 spray drone at different settings. Aspects of Applied Biology - International Advances in Pesticide Application 148, 19–29.